A sample holder for simultaneous neutron and dielectric spectroscopy -

dielectric tests with glycerol, glycerol-water, water and phosphoric acid

Bernhard Frick[1,*], *Margarita* Fomina[1,2,], *David* Noirat[1,3,], *Henriette W* Hansen[3,], *Markus* Appel[1,**], and *Kristine* Niss[3,***]

[1]Institut Laue-Langevin (ILL), CS 20156, F - 38042 Grenoble Cedex 9, France

[2]Jülich Centre for Neutron Science (JCNS) at Heinz Maier-Leibnitz Zentrum (MLZ), Forschungszentrum Jülich GmbH, Garching, Germany

[3]Glass and Time, IMFUFA, Department of Science and Environment, Roskilde University, Postbox 260, DK-4000 Roskilde, Denmark

Abstract. We report on dielectric test measurements of a rectangular flat sample holder which serves as capacitor and which is aimed for simultaneous neutron and dielectric (n-DE) spectroscopy of acidic liquid samples. We describe technical details of the sample holder assembly and the dielectric and neutron equipment as well as the sample preparation procedure of the air sensitive acidic samples. The sample holder was characterised off-line from the neutron spectrometer by dielectric spectroscopy, but using the standard IN16B cryofurnace with a dielectric sample stick with 4-wire connection and a Novocontrol - equipment, previously setup by a collaborative effort between ILL and Roskilde University. Temperature-dependent dielectric scans on standard samples (glycerol, glycerol-water, and Milli-Q water) were measured in the frequency range between 0.27 Hz and 1 MHz. Step-like temperature changes allowed to probe the temperature equilibrium conditions and continuous temperature changes were made to mimic typical IN16B backscattering neutron fixed window scans. Both type of scans were carried out in cooling and in heating. The standard samples show that our dielectric setup with flat sample holder is well suited for simultaneous n-DE-experiments. On the other hand, the dielectric scan on phosphoric acid reveals the limitations of our setup in case of high sample conductivities, but also shows that the DC-conductivity can still be accessed in a sufficiently wide low temperature range where the onset of conductivity can be simultaneously probed with the change in proton dynamics as seen by neutron spectroscopy.

1 Introduction

Quasielastic neutron scattering (QENS) [1] and dielectric spectroscopy (DES) [2] are complementary techniques and the application of both is of interest for many areas of science. QENS offers both time and space resolution for characterising molecular motions, whereas DES probes the time- or frequency dependence of electrical dipoles. QENS thus has the potential to inform about the type and time scale of atomic or molecular motions, like e.g. on the diffusional behaviour of ionic or non-ionic species. Regarding the dynamics of ionic species it is known that the QENS signal is not always straightforward related to charge displacements. In contrast DES can probe at lower frequency the DC-conductivity and at higher frequency the transition to AC-conductivity arising from the motion of ionic species. Thus it is obvious that a combination of the two techniques does give deeper insight and this has been widely used by comparing results from dedicated experiments applying these complementary techniques.

Standard broad band DES covers an extremely wide frequency range of more than 9 orders of magnitude in

a single experimental setup, like from the μHz to above-MHz region, whereas standard QENS offers typically only 2-3 decades between energy resolution and maximum energy transfer, thus requiring often a combination of different instruments or experimental setups. Even though these methods are probing different time scales, i.e. hundreds of seconds to 10^{-7}s for standard DES and 10^{-7}s to sub-picoseconds for QENS, it is in some cases of interest to carry out experiments simultaneously, in spite of evidence that dedicated individual experiments may deliver superior data quality. Scientific cases where simultaneous neutron and dielectric (n-DE) measurements are expected to give more information include i) non-equilibrium systems in general, ii) systems where a connection between low frequency dipole dynamics, probed by DES, and high frequency atomic motion, probed by QENS, is suspected, such as the hypothesis about a general connection between fast and slow dynamics [3], or more specific, iii) samples with crystallisation tendency or in metastable states which depend on the sample history, where it would be difficult to prepare the samples under exactly the same conditions in two separate experiments. Other more practical reasons could be parameter scans, like temperature or pressure scans, where kinetic delays between the measured

*e-mail: frick@ill.eu
**e-mail: appel@ill.eu
***e-mail: kniss@ruk.dk

parameter value and the actual intrinsic sample parameter value may differ and cause a non-equilibrium situation or samples with crystallisation tendency for which the interest is to measure with both methods exactly under the same conditions.

Simultaneous QENS and DES (called hereafter 'n-DE') experiments were started at the Institut Laue-Langevin some years ago by the group of K. Niss [4], mainly for n-DE experiments under pressure with a n-DE pressure cell allowing to access P=400MPa in a broad temperature range [5] and with Roskilde-owned DE-equipment (standard LCR meter 4284A from Agilent) from which emerged several publications (e.g. [6],[3],[7]). Recently, in continuation of this Roskilde-ILL collaboration, ILL has acquired a Novocontrol Alpha Analyser [8] which is now integrated into ILL's NOMAD data acquisition chain [9] and has built a sample stick with connectors for four-wire DES measurements fitting into the standard 50 mm diameter cryofurnaces and cryostats. Here we are reporting on tests of a flat sample holder, usable for ambient pressure experiments on acidic samples in a wide temperature range between T = 2 K and 340 K. We describe the sample holder assembly and off-line dielectric temperature scans, carried out under the same conditions and with the same equipment as found normally in fixed window scans [10] on IN16B [11]. As test samples we have chosen the well known (non-acidic) samples glycerol, glycerol-water and Milli-Q water, background reference samples as well as phosphoric acid water mixtures (PA-water) on which lies our main focus of future simultaneous n-DE experiments. We briefly describe the sample preparation procedure for the very air sensitive samples of PA and the practicality for user experiments. Dielectric scans were taken in a frequency range from 0.27 - 1 MHz and at temperatures between 2 and 340 K. Our tests show that our sample holder design is well suited for dielectric measurements at low temperatures as long as the sample conductivity and electrode polarisation is not too high. Both reduce the frequency and temperature range for measuring the conductivity with our dielectric setup. As our main interest of future work is to test at low temperatures for phosphoric acid - water mixtures a possible connection between the onset of conductivity (from the DC conductivity of DE spectra) and high frequency dynamics of proton displacement (from neutron fixed window scans, e.g. on IN16B or IN13), this restriction is acceptable.

2 Methods

2.1 Dielectric equipment and measured quantities

The dielectric equipment, which is available at ILL for simultaneous n-DE experiments [12], is based on a Novocontrol Alpha-AT Analyser, controlled by a PC running WINDETA software [8] and which can be triggered by the ILL instrument software NOMAD [9] to run simultaneous with the instrument data acquisition. With dedicated dielectric equipment the Novocontrol analyser covers a wide frequency range in the μHz- to above-MHz region.

Our test measurements were carried out in a restricted frequency range from 0.27 Hz to 1 MHz. The DE-analyser is connected via a dispatch box to an ILL built sample stick, which is more than 1 m high and is usable with standard ILL top loading 'Orange cryostats' having a 50 mm diameter bore. For our tests we have used the standard IN16B cryofurnace. The length of the sample stick and the sample orientation is adjustable and serves for placing the sample in the centre of the neutron beam. The cables for 4-wire measurements are fed through the central tube of the sample stick and are at their end welded in pairs to two pin connectors. These can then be plugged onto the pins fixed on the electrodes of any type of sample holder. The sample holder is connected with an intermediate electrically insulating PEEK adapter via an M8 thread to the end of the sample stick and is thus located just below the place where the sample temperature is measured.

A detailed description of broad band dielectric spectroscopy can be found in the book by Kremer and Schönhals [2]. DES derives the electrical properties from a measurement of the complex impedance Z* of a sample placed between electrodes. From the measured impedance one can find the complex capacity C* which is related to the geometry of the sample cell by $C \propto \frac{A}{d}$, with A being the sample area and d the sample thickness. Thus for DES a large sample area A and a small sample thickness d result in a large measurable signal. From the complex capacity C* of the sample cell one can derive the sample permittivity $\epsilon^* = \frac{C^*}{C_0}$, where C_0 refers to the empty sample cell capacity, and the complex dielectric permittivity is given by $\epsilon^* = \epsilon' - i\epsilon''$. From the complex permittivity one can then calculate the complex conductivity $\sigma^* = \sigma' + i\sigma''$, which is related to the complex permittivity by $\sigma^* = i\omega\epsilon_0\epsilon^*$ (ϵ_0 is the dielectric permittivity of vacuum).

2.2 Sample holder and requirements for simultaneous n-DE experiments

For neutron scattering basics we refer to standard books, e.g. [13], [14] or [1] and discuss only the requirements for a neutron sample holder. For maximum intensity the projection of the sample holder area A should cover the incoming neutron beam area, which on the instruments used is typically about 10 -30 mm wide and 20 - 50 mm high. The sample thickness should be chosen thin enough to favour single over multiple scattering processes. For that reason a rule of thumb is to aim for a scattering probability of less than 10% , equal to a transmission larger than 90% if absorption is neglected. For protonated materials, due to the high incoherent cross section from Hydrogen, a sample thickness d for straight neutron transmission should therefore be in the order of 150 μm and can be thicker for other samples. Both, A and d required for n-scattering, are thus compatible with the requirements for DES described above.

Two major sample geometries are used for QENS, a flat sample holder which can be oriented with respect to the incident and scattered neutron beam and thus with respect to the scattering vector **Q** and a hollow cylinder geometry for which the neutrons pass twice through the an-

nular sample thickness. There are standard designs for both types at ILL (and similar design elsewhere), which allow to adapt easily to different sample thickness.

We limit ourselves to the flat sample holder design which we have modified to suit simultaneous n-DE-spectroscopy. A cylindrical sample holder for n-DE spectroscopy will be described elsewhere [15]. For completeness we should mention an earlier sample cell development which was aimed for simultaneous neutron diffraction (different requirements than for QENS) and dielectric spectroscopy [16].

For adjusting to different sample thickness, one part of the sample holder remains usually unchanged and the counter part is slightly changing its dimensions: for flat sample holders it is the base of the holder which remains unchanged and top cover plates of different depth are used which dive into the base plate sample holder (see Fig.1) and leave a gap defining the desired sample thickness between 0 - 3 mm. The standard flat sample holders are made from Aluminium (small scattering cross section for wavelength below the Bragg cut-off) and can be sealed with Indium wire, squeezed in between the outer more massive frames which are held together by Aluminium screws. For dielectric spectroscopy these two parts of the sample holder (base and top) serve as electrodes.

Modifications which were made to this type of flat sample holder are the following 1: i) We have added by cold fitting tiny electrical connector pins on the upper edge of the two sample holder pieces. After screwing the sample holder to the sample stick, these allow to connect the wires for the DE- measurement. ii) We isolate electrically the electrodes (top and base) from each other by thin Teflon sheets on which the central part is cut out in order to leave most of the neutron window free. When closing the sample holder, the top cover pulls the thin teflon foils into the base plate so that it is lining equally the side walls of the sample volume. We have used 2 or 3 such very thin window foils of only $10\mu m$ thickness. This minimises the risk of shearing off the teflon foil when closing the sample holder. It also minimises the neutron background arising from the coherent scattering (Bragg peaks) of Teflon (PTFE), which is important because minor parts of the foil near the border of the neutron window might still reach into the neutron beam. iii) For sealing liquid samples we squeeze an Indium wire, placed in between the foils around the sample volume. The PTFE foils also protect the Indium from contact with the sample as we aim for measuring acidic liquids. At first Aluminium screws are used for sealing the sample cell (squeezing the Indium wire), which after tight closing are then exchanged one by one by electrically insulating Nylon screws. iv) Our aim is to measure acidic samples which would corrode the Aluminium quite fast. Therefore the neutron windows with their side walls were coated on the inside of the sample holder with a very thin Au layer ($0.34\mu m$) in order to minimise neutron activation of the sample holder. v) As the major source for potential neutron background stems from the nylon screws (protonated carbon chain) we attach, for the neutron scattering experiments only, a Cadmium mask on top of the sample holder facing the neutron beam, tak-

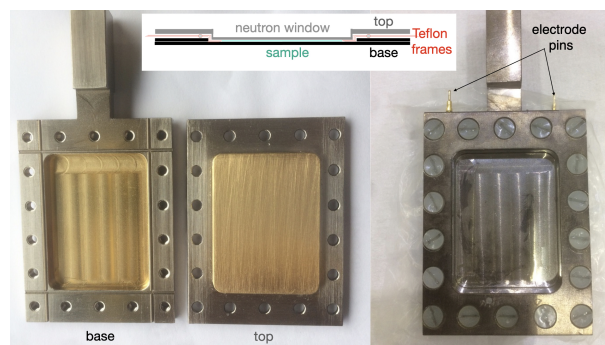ing care not to create electrical contact between the electrodes.

Figure 1. left photo: gold coated sample holder: bottom part (l.h.s.) and top cover (r.h.s.); right photo: filled sample holder with Nylon screws and electrode pins on top. Inset: schematic view how the sample is squeezed between base and top plate and how the 3 thin Teflon foils are placed.

2.3 Sample preparation

All air sensitive samples were handled within a glove bag under Argon flow, including in a few cases melting the crystalline samples on a heat plate, weighing the appropriate sample amount and pipetting it into the sample holder. Sample handling took place only after a low humidity level had been reached (typically 2.5% RH at about 20C). RH and temperature were registered continuously close to the sample with a Sensirion humidity sensor. The exposure time of the samples to the dry atmosphere was minimised to several ten seconds until the sample holder was closed and initially kept together with a special tool until it was definitively closed with screws outside of the Argon bag.

Critical and delicate phases are the preparation of the sample holder with the very thin Teflon foils and the Indium wires in between, the transfer of this assembly to the glove bag, and the closing of the sample holder within the bag, where the foils are hardly anymore visible. During closing the sample holder with screws, care had to be taken not to pull the Teflon foils with the screws into the threads which could rupture the foils and create electrical contact. Punching holes into the very thin foils before assembly seemed difficult, therefore we have perforated the foils with a needle in the center of each screw hole after assembly and then placed the Aluminium screws. In some cases a short circuit was detected after the sample assembly and then the described tedious procedure had to be repeated. In that respect there is room for improving the sample holder design and handling.

3 Dielectric tests on standard samples

In order to test our sample holder design we have carried out dielectric spectroscopy on well known samples and on empty sample holders in the IN16B standard cryofurnace and with the sample stick described above. As test samples

we have used Milli-Q-water, glycerol and a glycerol-water mixture. Finally we report on a phosphorous acid - water mixture, belonging to the group of samples which meet closest our main objective, namely measuring the low temperature conductivity of PA-water systems simultaneously with neutron spectroscopy. Systematic measurements on this series will be reported elsewhere. Here we show that our experimental setup is well suited for dielectric measurements on standard samples. But we also point out the experimental limitations of our setup for samples with extremely high conductivity similar to that of PA.

3.1 Tests on glycerol

As an example for the DE-data quality achievable with our n-DE-setup we show in Fig.2 dielectric spectra measured in a frequency range from $2.7 10^{-1} - 10^6$ Hz on glycerol between 209 K and 240 K at temperatures similar to the ones reported in literature (e.g. [17]) which show the α-relaxation peak in the imaginary part of the dielectric permittivity ϵ''.

For two temperatures (T = 209 K and 219 K) we show in Fig.3 fits of the α-relaxation peak observed in the imaginary part of the dielectric permittivity ϵ'' of glycerol. We have fitted ϵ'' applying a single Havriliak-Negami (HN) model fit function with an additional conductivity term, resulting in HN shape parameters $\beta = 0.97$ and $\gamma = 0.48$. β is found to be very similar to the value given in Ref.[2] ($\beta = 0.95$), but the smaller γ found by us ($\gamma = 0.6$ in Ref.[2]) indicates a lower slope in the high frequency wing. We attribute this to the fact that we have not fitted an additional HN-function to the high frequency wing as it was done in Ref.[2].
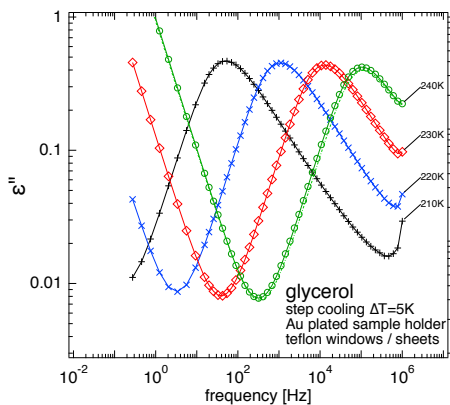

Figure 2. Frequency dependence of the imaginary permittivity of a glycerol sample, measured in a gold coated flat sample holder, placed in an IN16B cryofurnace, suited for simultaneous neutron scattering.

In neutron spectroscopy a powerful way to get an overview over the onset of different relaxation processes as a function of the sample temperature or pressure are so-called (elastic or inelastic) fixed window scans (EFWS, IFWS, FWS) [10]. Such FWS are most efficiently carried out on reactor backscattering spectrometers using a linear-motor Doppler drive, where the incident neutron
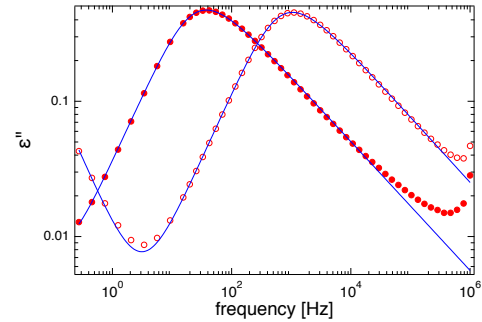

Figure 3. Test fits with a HN-function including conductivity of the α-relaxation peak of glycerol at T = 209 K and T = 219 K.

wavelength $\lambda_{inc}(t) = \lambda_M \pm \Delta\lambda_D = \lambda_M \mp \frac{h}{m_n} \frac{1}{v_D(t)}$ can be flexibly set offset with respect to the fixed wavelength $\lambda_M = \lambda_A$ of the static monochromator and the analysers by choosing an appropriate periodic Doppler velocity profile $v_D(t) \approx \pm const.$ for the backscattering monochromator which, when discarding the regions near the reversal points, is constant [10].

This way most of the neutron detection time is spent in the corresponding energy transfer channel $E = \frac{\hbar^2}{2m_n}((1/\lambda_A)^2 - (1/\lambda_{inc})^2)$ which is probed with sub-μeV energy resolution and thus with the longest relaxation times currently available on neutron spectrometers operating in frequency space. In view of the short neutron measuring times and the superior statistics of FWS compared to QENS, carrying out the fast DE-spectroscopy simultaneously with FWS might be of highest interest (e.g.[18]).

In order to prepare for such n-DE-experiments we have carried out off-line temperature scans on glycerol in cooling from 330 K to 15 K with a continuous cooling ramp of -0.5 K/min (see Fig.4a), followed by continuous heating (Fig.4b) with the same ramp speed of 0.5 K/min using a gold plated flat sample holder and the IN16B standard cryofurnace. In a ramp the sample temperature set point was adapted continuously every 6 seconds. A frequency sweep for the dielectric spectra was chosen to last about 2 min in the range 0.2 to 1 MHz, followed by a waiting time of 1 min, which should be compared with neutron measuring times (not reported here) of about 30 s for an EFWS and 60-180 s for an IFWS step. The time for a DE frequency sweep would become much longer and would no longer match a temperature step of the FWS if lower frequencies were chosen (e.g. one period at 1 μHz equals 1000 s).

For both sets of scans it can be seen in Fig.4 how the -relaxation peak moves in the intermediate T-range through the dielectric frequency window. With increasing temperature the spectra are dominated towards lower frequency by strong DC conductivity leading to $\epsilon'' \propto 1/\omega$. The spectra in Fig.4 show also the limitations of our experimental setup at low temperatures and at frequencies above 10^5 Hz where the systematic errors increase (see also empty can measurements). Some temperatures are highlighted by colours to show their different behaviour.
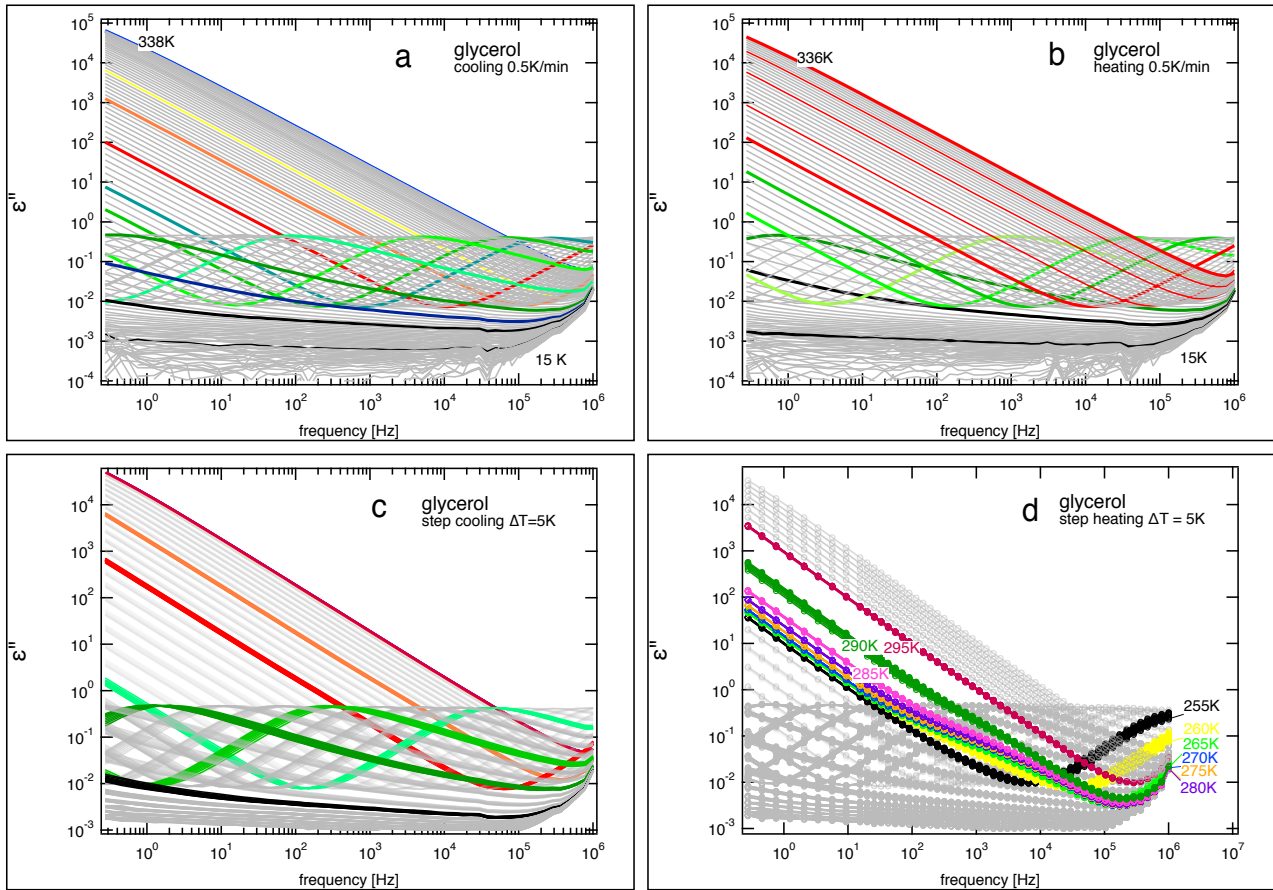
Figure 4. Frequency dependent dielectric permittivity at temperatures measured in: (a) continuous cooling scan with a ramp of 0.5 K/min, (b) continuous heating with the same rate, (c) in step cooling with ΔT=5K, followed by scans during temperature equilibration and (d) in step heating, followed by scans during temperature equilibration. With the slower rate in step heating crystallisation of glycerol is observed.

Depending on the heating or cooling rate a temperature equilibrium at the sample may not always be guaranteed. This depends on the details of the experimental setup and in our case the thermal equilibration is prolongated with respect to normal FWS conditions on IN16B because an electrically and thermally insulating PEEK adapter is placed between the sample and the sample stick (see experimental details). In order to get information on temperature equilibration we have also carried out measurements in step cooling and heating with much longer temperature equilibration times. We judge the equilibration time from the dielectric sample response which is recorded for a nominally identical sample temperature. Such step scans, which followed without sample change the continuous temperature scans (Fig.4a,b), are shown in Fig.4c and Fig.4d. Here the temperature set point was lowered or increased in steps of ±5 K. After a waiting time of 10 min a frequency sweep of the dielectric signal was recorded which took about 2 min and was repeated ten times before changing to the next sample set point temperature.

From Fig.4c) it seems that the sample reaches thermal equilibrium faster at higher temperatures than at low temperatures near the glass transition of glycerol ($T_g \approx 185K$), which could be a kind of aging effect. It might, however,

as well reflect that at low temperatures, when approaching the glass transition, an equivalent sample temperature change causes a larger frequency shift of the ϵ'' signal than at higher temperature. In fact the data points in the temperature plot of Fig. 5 below are more spread in the α-peak region where the most pronounced temperature shift is expected on ϵ''.

During the step heating scans of glycerol (Fig.4d) a somewhat different behaviour was found, which is highlighted by the coloured curves. A nearly temperature independent shoulder developed near 260 K in the frequency range $10^2 - 10^5$ Hz, followed by a major rapid increase of ϵ'' in the whole frequency range near 290 K. We ascribe these features to (partial) crystallisation phenomena, followed by melting at higher temperatures in heating. The equilibrium melting temperature for glycerol from literature is about $T_m = 291K$. In cooling or in the faster continuous heating glycerol doesn't show any sign of crystallisation in our measurements.

A detailed analysis of the crystallisation kinetics of glycerol by DE-spectroscopy with dedicated equipment can be found elsewhere (see e.g. Ref.[19],[20] and references therein) and is not the purpose of the present paper. We don't offer a quantitative analysis of the glyc-
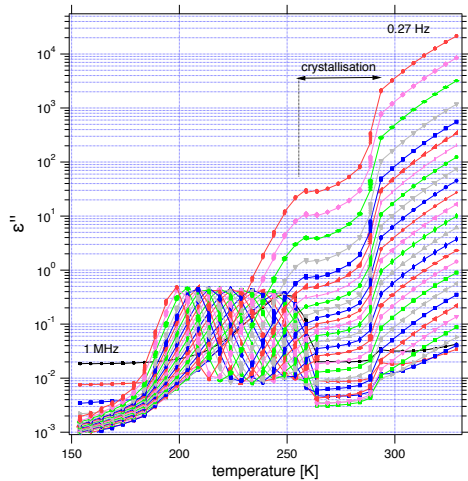
Figure 5. Temperature dependence of the dielectric permittivity of glycerol at selected frequencies measured in step heating.
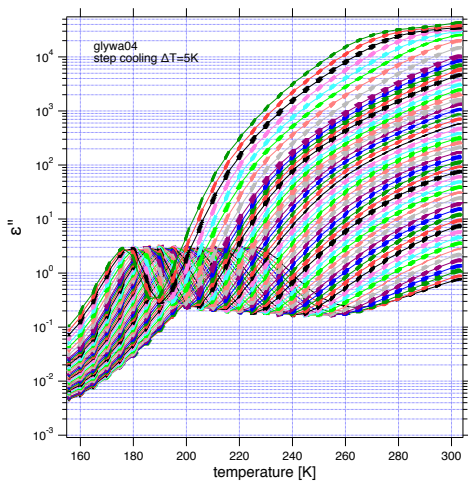

Figure 6. Temperature dependence of the dielectric permittivity of a glycerol-water mixture with a 0.4 molar fraction of glycerol as measured in step cooling.

erol signal but only strengthen our hypothesis that we observe (partial) crystallisation by plotting the temperature dependence at different constant frequencies between 0.27 Hz and 1 MHz (Fig.5). The temperature at which the α-relaxation peak maximum is observed in heating is strongly frequency dependent as expected; it is located near 200K for 0.27 Hz and near 250 K for 1 MHz. With the thermal protocol applied in our study glycerol crystallises near 260 K indicated by a frequency independent feature in Fig.5, a temperature region in which ϵ'' increases only moderately compared to the temperature increase below 260 K. At the end of this crystallisation region, near the melting temperature T_m = 291 K, ϵ'' jumps back to a higher value which can be considered as the extrapolation of the ϵ'' values below the crystallisation region.

3.2 Tests on glycerol-water

A detailed study of the glycerol-water system by DE and neutron spectroscopy as a function of both temperature and pressure is part of a PhD thesis by D.N. [15]. For testing our setup we show here the measurement on a glycerol-water sample with 0.4 molar fraction of glycerol in our flat sample holder, following the same protocol as described for neat glycerol described above. No crystallisation was observed in any of the cooling or heating scans. Fig.6 shows the corresponding temperature dependence for all measured frequencies between 0.27 Hz and 1 MHz and for step cooling with ΔT = 5 K.
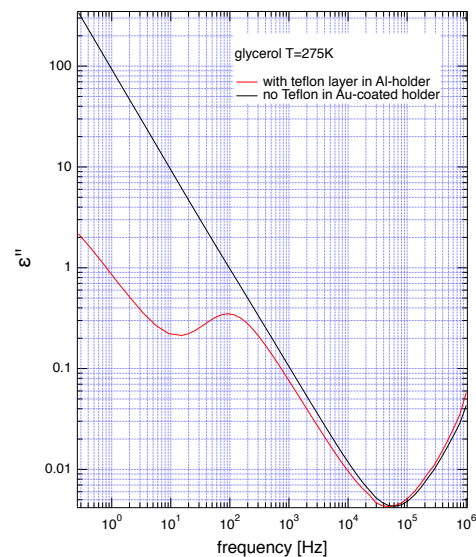
3.3 Influence of Teflon

Figure 7. Imaginary part of the dielectric permittivity of glycerol with and without a Teflon covered electrode. A peak appears with Teflon coverage as discussed in the text. ϵ'' for glycerol with standard Teflon windows (black curve) is scaled down by 0.55 to match roughly the minimum seen near $5 \cdot 10^4$ Hz

There is some discussion in literature about the possibility to cover one electrode with a teflon layer for extracting a signal which might be hidden below a high DC-conductivity contribution ('blocking electrode') as published for glycerol by Bergman [17] and commented by Ref.[21] with reply by Ref.[22]. We are not aiming to contribute to this controversial discussion. But for our n-DE-sample holder we used Teflon foil frames for electrical insulation between the electrodes (2 or mostly 3 foils, thus 20 or 30 μm in total) with nominally no Teflon in the neutron window, but only sample (see inset in Fig.1). However, assuming that the 3 foils may not always be perfectly superposed, there could be a possibility that a little part near the edge of the neutron window (capacitor) of our sample holder might have a 10 μm teflon with some sample on one or both sides. Thus we have tested by purpose to increase the electrode coverage with teflon by decreasing drastically the window size which we cut into a single

10 μm thick teflon foil (in the order of 1 cm^2 window). We show in Fig.7 that in that case we detect a peak with the partially teflon covered electrode, which is absent if we use our standard Teflon frames with proper opening as described in ch.2.2. This check and the absence of such a peak is important for our data measured on PA-water, which we will discuss below.

3.4 Tests on Milli-Q water

As another characterisation of our nDS setup we have measured pure Millipore water (see Fig.8). The imaginary permittivity versus frequency, measured in continuous cooling with 0.5 K/min, changes abruptly from a smooth frequency dependence at temperatures above a registered sample temperature of 266.6 K to curves exhibiting at least one peak, which moves with further cooling to lower frequencies. We assign this observation to a freezing of the supercooled milliQ water in this type of cooling scan and at lower temperatures the observation of relaxation peak(s) in ice. In heating with 0.1K/min the melting is found near T = 273K as shown in Fig.8, r.h.s.

Similar to glycerol we have carried out in a limited temperature range on MilliQ-water DE-scans in step cooling (Fig.8c, bottom, l.h.s.) and also during much slower continuous heating with 0.1 K/min (Fig.8c, bottom, r.h.s.)), which confirm the presence of relaxation peaks in the crystal. As the empty sample holder does not show such peaks and as we didn't see relaxation peaks with teflon in the normal setup on glycerol, we can be fairly sure that the small peaks seen at low temperatures in the ϵ''-signal stems from ice water.

3.5 Comparison of the empty holder with glycerol

In order to get an indication of how much the empty sample holder may contribute to the measured ϵ''-signal we have measured an empty sample holder prepared in the same way as the filled samples, but on air. In these measurements the ϵ''-signal of the empty cell (lines in Fig.9) was smaller than 10^{-3} and thus significantly lower than the permittivity of glycerol (symbols in Fig.9) measured under similar conditions. The empty cell signal decreases with decreasing temperature. At high frequencies we see for all temperatures an increase of ϵ'' towards 1 MHz, the upper limit of the frequency range we decided to probe, ending in a similarly high ϵ'' value.

3.6 Tests on PA-water

All DE-measurements reported in the previous sections were carried out on standard samples and suggest that our sample holder design should be suited for simultaneous neutron and dielectric spectroscopy. As our project aim is to measure on phosphoric acid - water (PA-w) mixtures simultaneously conductivity spectra by DE-spectroscopy and proton dynamics by n-spectroscopy, we show here an example of the DE-scans taken on PA with our n-DE-setup. We refer the discussion concerning the physics of PA and PA-w-mixtures to a later publication and discuss
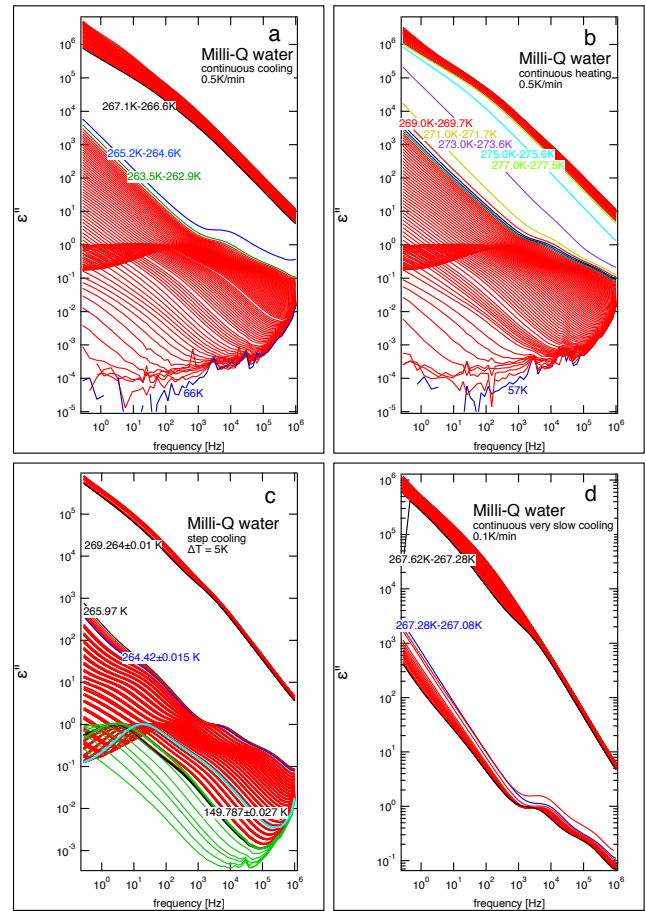

Figure 8. Imaginary part of the dielectric permittivity of Milli-Q water, measured during temperature scan in continuous cooling and heating with rates of ± 0.5 K/min (top), in cooling with steps of ΔT = 5K followed by equilibration (bottom, left) and around the melting / crystallisation with a slower cooling ramp of 0.1K/min (bottom/right).

here the limitations of our setup which we found on theses systems at high temperatures and high sample conductivity. As a note in passing we mention that phosphoric acid (PA) is known to exhibit an extremely high intrinsic proton conductivity, which can be further enhanced only by the addition of water (see e.g. [23], [24], [25]).

In Fig.10 we show dielectric spectra taken on dry PA. We observe for PA and PA-water mixtures (not shown here) at high temperatures a sharp decrease of the imaginary part of the permittivity ϵ'' in the high frequency range (highlighted within the dashed frame in Fig.10), which is not present at lower temperatures. In Fig.10 and the following we explain why the apparent peak formed is most probably an artefact. This is also suggested by the real part ϵ', which decreases sharply and which takes on negative values at high frequency and high temperatures (for frequencies above the vertical dashed line). This becomes more clear by plotting for 271 K additionally the modulus of ϵ', shown by the dots in the upper part of the figure.

To underline this we add a figure with the measured impedances Z, where Z'_s and Z''_s corresponds to the serial real and imaginary part of the impedance as it is output by
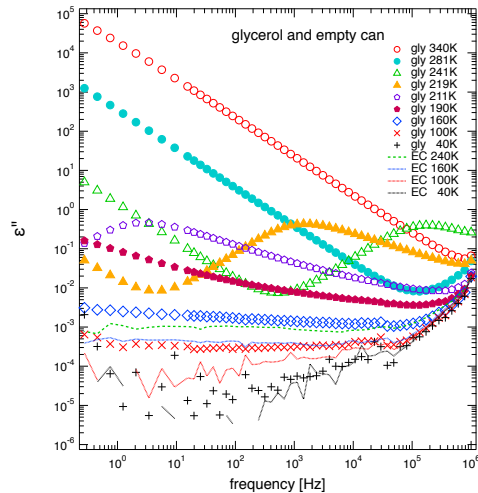
Figure 9. Dielectric scan on empty can (lines) and glycerol (symbols) for comparison are shown at several temperatures (see legend; same colour indicates same temperature).
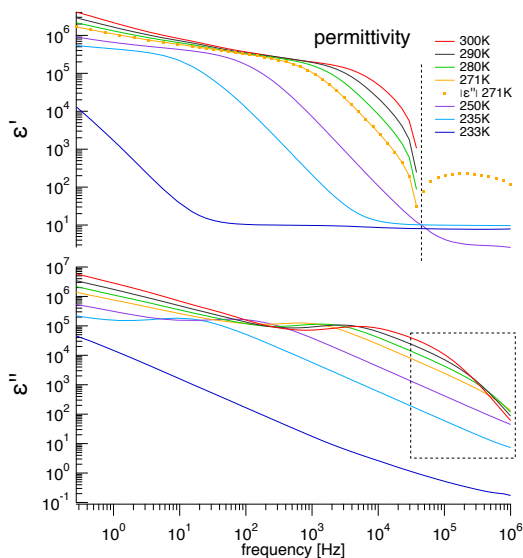

Figure 10. Real and imaginary part of the dielectric permittivity of phosphoric acid (PA), measured in cooling with the setup for simultaneous n-DE-spectroscopy and showing anomalies for high temperatures at high frequency. For ϵ'' we find at high frequency with increasing temperature an increasingly steeper decay (lower figure; dashed square region). In the same temperature-frequency region the real part of the permittivity ϵ' turns negative (upper part: r.h.s. of the dashed line). As the data are plotted on a log-log scale, we have highlighted this by adding for 271 K the absolute values of ϵ' (dots). Note also that crystallisation has appeared between T = 235 K and 233 K.

Figure 11. Impedances Z as measured on phosphoric acid (PA) with the setup for simultaneous n-DE-spectroscopy. Upper figure: real part of the serial impedance Z'_s. Lower part of the figure: imaginary counterpart Z''_s which changes sign at the frequency indicated by a dashed vertical line (positive at high and negative at low frequencies). Dots in the lower figure correspond to the absolute value of Z''_s shown for T = 300 K only.

tion contributions from the cables might become important, in spite of the 4-wire connection. It is known that it may be difficult to measure highly conducting liquids by dielectric spectroscopy, especially at higher frequency, if the measuring cell is not suited [8]. For DE-spectroscopy a much larger spacing between the electrodes can then be chosen, which however would conflict, at least for protonated samples, with the requirement of simultaneous neutron spectroscopy for which the thickness should be chosen to minimise multiple scattering.

Another possibility which we can't exclude completely as explanation of this artefact could be that our Teflon frames could produce a peak in ϵ' as discussed above in section 3.3 and in Ref.[21]. However, as the temperature scans were measured in cooling, we can expect that the sample geometry (rearrangement of electrodes/Teflon/sample which might depend on viscosity) does not change when cooling to lower temperature and therefore the same feature would be visible as well at lower temperature. These described artefacts unfortunately limit the useful frequency range at high temperatures and for high conductivies for our planned PA-water measurements.

Nevertheless, as can be seen by calculating the conductivity σ' in Fig.12, we are able to determine well the DC-conductivity plateau level with our simultaneous n-DE-setup. Thus we will be able to deduce valuable information by comparing the temperature and water concentration dependence of the DC-conductivity plateau with the neutron scan data, even though it would have been better to see the transition from DC- to AC- conductivity in

the Novocontrol WINDETA [8]. Z''_s changes from negative to positive sign above this frequency as shown in the lower part of Fig.11.

As the onset of the ϵ''-decrease with frequency varies systematically with conductivity, i.e.with increasing temperature and with increasing water content, we suspect that due to the extremely high conductivity of PA-water induc-
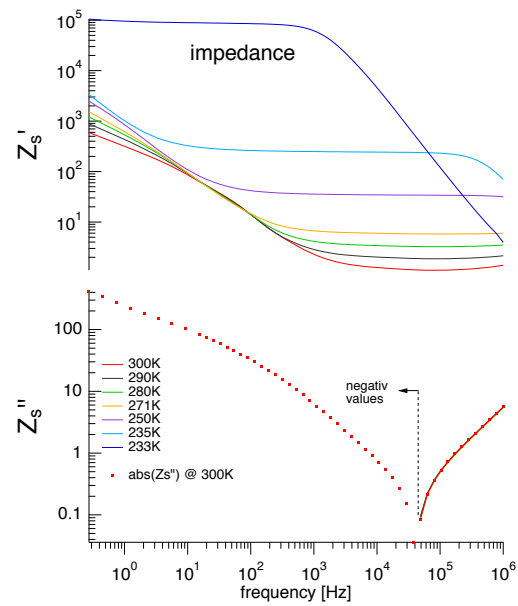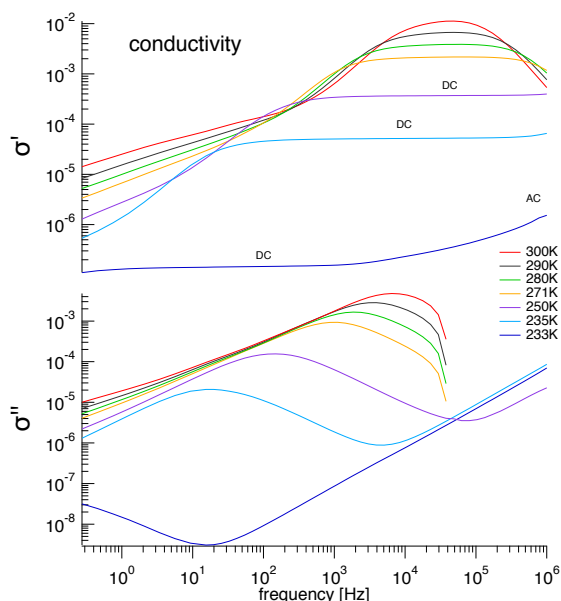
Figure 12. Conductivities as measured on phosphoric acid (PA) with the setup for simultaneous n-DE-spectroscopy. Upper figure: real part of the conductivity σ' and lower part of the figure the imaginary part σ''

a wide frequency range. Such simultaneous comparison is important as we have shown above by step cooling that temperature equilibration can be long and that temperatures recorded in the continuous cooling or heating FWS scans are no equilibrium sample temperatures.

4 Conclusion

We have presented a design for a flat sample holder which can serve as a sample cell (capacitor) for dielectric spectroscopy and in which the same sample volume permits scattering neutrons, thus allowing for simultaneous neutron spectroscopy. The presented type of sample holder allows for measuring normal, air sensitive and acidic liquids, i.e. it is a sealed sample cell which we assembled for some samples in a dry Argon atmosphere - noting that this operation is delicate. The upper temperature range is limited by the Indium seal to about 340K. Dielectric test scans in a wide frequency (0.27 Hz - 1 MHz) and temperature range (2 K - 340 K) on several standard samples (glycerol, water, glycerol-water) and under conditions similar to neutron fixed window scans (FWS) show that our flat cell design, in connection with ILL's DE-equipment, is working well, albeit not being competitive with a dedicated DE-spectroscopy or a dedicated neutron scattering setup, which is what we had expected.

We have pointed out some limitations of our n-DE-setup comprising the empty cell, like systematic errors which become important at higher frequencies. For samples with very high conductivity, like the PA sample tested in this work, another severe restriction in the high frequency range is observed at high temperatures. We ascribe this to the inductivity of cables becoming important for high sample conductivity.

Another limitation which we should stress is that absolute values of the dielectric permittivity or the conductivity are difficult to obtain with our setup. This can be judged e.g. from Fig.2 and Fig.3 were the permittivity of glycerol is found to be lower than regularly reported in literature. Although somehow expected, taking into account that we don't use a dedicated dielectric spectroscopy equipment, it is instructive to learn about the most probable reasons. Certainly the sample holder, originally designed for neutron scattering only, adds a non-negligible contribution as we have shown. Another important contribution comes from imperfect sample filling, which is nearly unavoidable with the present design but which could have been further optimised for the glycerol data shown. The sample is filled in the liquid state near room temperature and the needed sample quantity is calculated from the nominal sample holder dimensions. However, mechanical precision and the necessary play between the top and bottom pieces, uncertainties in the sample thickness due to the squeezed Indium seals and Teflon or minor deformation of the thin Aluminium neutron windows will contribute mostly to underestimate the sample quantity needed. Thus some void or gaz filled volume and an imperfect sample geometry are difficult to avoid and cause more problems for highly viscous samples. Thus one should be aware of the uncertain absolute value of the dielectric permittivity and envisage a more quantitative determination of the deviations in cases where it seems necessary.

In summary, the presented flat sample cell and setup for n-DE-spectroscopy will allow us tackling problems where simultaneous spectroscopy is of interest and we hope that the tests which we report here will help to develop a further improved generation of sample cells for simultaneous n-DE-spectroscopy.

References

[1] M. Bée, *Quasielastic neutron scattering: principles and applications in solid state chemistry, biology and materials science* (Adam Hilger, 1988)

[2] F. Kremer, A. Schönhals, *Theory of Dielectric Relaxation Spectra in Broadband Dielectric Spectroscopy* (Springer: Berlin, 2002)

[3] H.W. Hansen, A. Sanz, K. Adrjanowicz, B. Frick, K. Niss, Nature Communications **9**, 518 (2018)

[4] K. Niss et al., 10.5291/ILL-DATA.LTP-6-7 (2015)

[5] A. Sanz, H.W. Hansen, B. Jakobsen, I.H. Pedersen, S. Capaccioli, K. Adrjanowicz, M. Paluch, J. Gonthier, B. Frick, E. Lelièvre-Berna et al., Review Of Scientific Instruments **89**, 023904 (2018)

[6] H.W. Hansen, B. Frick, S. Capaccioli, A. Sanz, K. Niss, The Journal of Chemical Physics **149**, 214503 (2018)

[7] H.W. Hansen, F. Lundin, K. Adrjanowicz, B. Frick, A. Matic, K. Niss, Physical Chemistry Chemical Physics **137**, 080901 (2020)

[8] *WinDETA 6.02 - Program's Manual*, Novocontrol Technologies Germany (2017)

[9] *https://www.ill.eu/users/support-labs-infrastructure/instrument-control-service/remote-instrument-control* (last viewed 2022)

[10] B. Frick., J. Combet, L. van Eijck, Nuclear Instruments & Methods In Physics Research Section A-Accelerators Spectrometers Detectors And Associated Equipment **669**, 7 (2012)

[11] *https://www.ill.eu/in16b* (last viewed 2022)

[12] K. Niss et al (to be published)

[13] G. Squires, *Introduction to the Theory of Thermal Neutron Scattering* (Cambridge University Press, 1978)

[14] S. Lovesey, *Theory of neutron scattering from condensed matter* (Clarendon Press: United Kingdom, 1984)

[15] D. Noirat, *PhD thesis Roskilde University* (in progress)

[16] M. Jiménez-Ruiz, A. Sanz, A. Nogales, T. Ezquerra, Review of Scientific Instruments **76**, 043901 (2005)

[17] R. Bergman, H. Jansson, J. Swenson, The Journal of Chemical Physics **132**, 044504 (2010)

[18] H.W. Hansen, B. Frick, T. Hecksher, J.C. Dyre, K. Niss, Physical Review B **95**, 104202 (2017)

[19] A. Sanz, K. Niss, Crystal Growth & Design **17**, 4628 (2017)

[20] A. Sanz, K. Niss, The Journal of Chemical Physics **146** (2017)

[21] M. Paluch, S. Pawlus, K. Kaminski, The Journal of Chemical Physics **134**, 037101 (2011)

[22] R. Bergman, H. Jansson, J. Swenson, The Journal of Chemical Physics **134**, 037102 (2011)

[23] K.D. Kreuer, Chemistry Of Materials **17**, 610 (1996)

[24] J-P. Melchior, K-D. Kreuer, J. Maier, Physical Chemistry Chemical Physics **19**, 587 (2016)

[25] J-P. Melchior, B. Frick, Physical Chemistry Chemical Physics **19**, 28540 (2017)